Shell effects in Pb(p,xn) preequilibrium neutron emission

K. Harder, A. Kaminsky, E. Mordhorst, W. Scobel, and M. Trabandt
I. Institut für Experimentalphysik, Zyklotron, Universität Hamburg,
D-2000 Hamburg 50, Federal Republic of Germany
(Received 24 February 1987)

The ^{204,206,207,208}Pb(p,xn) reactions have been investigated at $E_p = 25.5$ MeV. The hard energy spectra and the structures observed in the preequilibrium continuum are attributed to the nearby double shell closure. Application of semiclassical preequilibrium models requires the reduction of the state density g and/or the use of $(1p)(1n)^{-1}$ state densities based on realistic single particle level schemes.

Preequilibrium (PE) nucleon emission from light ion induced reactions involves mostly only a few degrees of freedom. Most semiclassical PE models, though conceptionally different, share in a few basic ingredients that lead to a formal similarity. Their degrees of freedom are of single particle type and are referred to as excitons; the equilibration is attained through intranuclear quasifree nucleon-nucleon collisions; the grouping of configurations in terms of single particle excitations of growing complexity is described by the number of excitons n participating in the exciton energy E^*.

The formal similarity of two of these models—the exciton and the hybrid model—has been thoroughly examined with respect to the conceptional differences.[1] Here, it is only of interest that both models apply partial densities $\omega_n(E^*,\mathrm{p},\mathrm{h})$ of n exciton states composed of p particles and h holes to describe the exciton distribution functions $\rho_i(E^*,\epsilon_\mathrm{p},\mathrm{p}_i,\mathrm{h}_i)$. The state densities are of Ericson-Williams type[2] and are of key importance for the shapes of the resulting nucleon energy spectra.

It is the purpose of this work to demonstrate the influence of gross deviations of the partial state densities due to shell effects on both, experimental and calculated spectra. We have studied the sequence of reactions ^{204,206,207,208}Pb(p,xn) approaching (for $x=1$) the residual nucleus ^{208}Bi with a ground state having a $(1p)(1n)^{-1}$ structure beyond doubly closed shells. Such configurations are predominantly[1] populated by PE emission in (p,n) reactions. Calculations will be performed with the hybrid model[3] in the notation of Ref. 1. This work supplements and completes work previously reported by some of the present authors.[4,5]

The experiment has been performed with the 25.5 ± 0.15 MeV proton beam of the Hamburg Isochronous Cyclotron impinging on isotopically enriched, self-supporting targets of areal density 5.4 mg/cm^2 (^{204}Pb), 10.9 mg/cm^2 (^{209}Pb), and 20.2 mg/cm^2 (^{207,208}Pb). The neutron time-of-flight (TOF) set up consists of eight detectors (10 cm diam$\times$5 cm cylindrical cells of NE213) and flight paths of standard lengths between 7 and 8 m. Three optional target positions in front of, between, and behind two target magnets allow to cover the range $3^\circ \le \Theta_\mathrm{lab} \le 177^\circ$ with 24 roughly equidistant reaction angles. The geometry of the whole set up and the performance of the detectors have been described in detail elsewhere.[6,7]

The following experimental details are specific to this Pb(p,xn) experiment. The stop signal of the TOF measurement was derived from the stabilized[8] cyclotron radio frequency such that an overall and long term time resolution of 1.5 ns [full width at half maximum (FWHM)] corresponding to a neutron energy resolution of 60 keV (500 keV) for $E_n = 5$ MeV (20 MeV) could be obtained. In order to ameliorate this resolution, the TOF paths for two of the forward detectors were extended from 7.5 to 20 m. In addition, their scintillator cells were replaced by larger ones (25 cm diam$\times$5 cm). They allow to cover the angular range $\Theta_\mathrm{lab} \le 60^\circ$ ($\Theta_\mathrm{exp} = 9^\circ$, 15°, 27°, 33°, 47°, and 53°) with an improved energy resolution $\Delta E_n = 30$ keV (250 keV) at $E_n = 5$ MeV (20 MeV). Each run was followed by a background run with shadow bars being placed midway in the TOF paths.

Representative TOF spectra for a long flight path are given in Fig. 1. The time resolution of the analog resonance (IAR) is in agreement with the values quoted. The background subtraction represented at most a 10% correction of the integral yield in the physical region $E_\mathrm{bias} \le E_n \le E_n^\mathrm{max}$. After background correction the TOF spectra were converted into center-of-mass energy spectra of bin size $\Delta E_n = 100$ keV. From the resulting four sets of 24 energy spectra one can calculate for each bin the double differential cross sections for isotopically pure material. The angular distribution for selected energy bins in the regions with dominant PE contributions show the well known shapes and shall not be discussed here. Instead we focus attention on the angle integrated energy spectra that are shown in Fig. 2. The most striking features are as follows: (i) a great similarity in general shape combined with a moderate increase of the absolute values with mass number A in the PE continuum, at least for the region with residual excitation $U \ge 5$ MeV; (ii) structures in the region $U \le 5$ MeV that are the more pronounced the heavier the target isotope is.

In the subsequent discussion we want to correlate these observations with the approach of the residual nucleus $^{208}_{83}$Bi and its particular nucleon configuration. For this

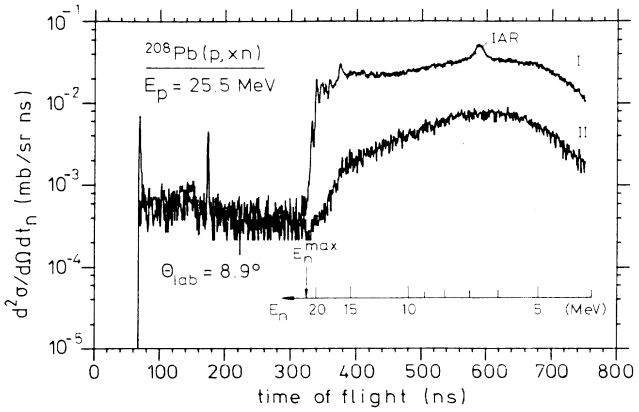

FIG. 1. Neutron TOF spectra for ^{208}Pb(p,xn), $\Theta_{lab}=8.9°$, and 20 m flight path, without (I) and with (II) shadow bar.

purpose we remind of the hybrid model,[3] in which the angle integrated spectrum of neutrons (ν) emitted with channel energy ϵ_ν is given by

$$\frac{d\sigma(\epsilon_\nu)}{d\epsilon_\nu}=\sigma_R\sum_i D_i\rho_i(E^*,\epsilon_{\text{s.p.}},\mathrm{p}_i,\mathrm{h}_i)\frac{\lambda_c(\epsilon_{\text{s.p.}})}{\lambda_c(\epsilon_{\text{s.p.}})+\lambda_+(\epsilon_{\text{s.p.}})}\ . \tag{1}$$

The sum extends over the exciton generations labeled i, starting with the one proton and one neutron particle, one neutron hole states, i.e., $\mathrm{n}_0=3$, $\mathrm{p}_0=2$, $\mathrm{h}_0=1$. The depletion of the reaction system, originally formed with the cross section σ_R, is taken care of with the factors $D_i<1$. Only single particle states with the excitation $\epsilon_{\text{s.p.}}\le E^*$ contribute. The rates $\lambda_c(\epsilon_{\text{s.p.}})$ for nucleon emission are calculated from the reciprocity theorem, those of the competing thermalizing collisions, $\lambda_+(\epsilon_{\text{s.p.}})$, from quasifree nucleon-nucleon scattering.

The exciton distribution functions $\rho_i(E^*,\epsilon_{\text{s.p.}},\mathrm{p}_i,\mathrm{h}_i)$ represent the probability of finding an exciton at excitation $\epsilon_{\text{s.p.}}$ in the ith generation, with p_i and h_i incremented[1,3] as $\mathrm{p}_i=\mathrm{p}_{i-1}+1$, $\mathrm{h}_i=\mathrm{h}_{i-1}+1$. The ρ_i are calculated under the assumption that each possible configuration of n_i excitons is populated with equal probability, yielding

$$\rho_i(E^*,\epsilon_{\text{s.p.}},\mathrm{p}_i,\mathrm{h}_i)=\frac{g\omega_{n_i-1}(E^*-\epsilon_{\text{s.p.}},\mathrm{p}_i-1,\mathrm{h}_i)}{\omega_{n_i}(E^*,\mathrm{p}_i,\mathrm{h}_i)}\ . \tag{2}$$

Whereas the partial n_i exciton state density ω_{n_i} only influences the absolute value of the ith contribution, ω_{n_i-1} is of importance for its shape and, to a lesser extent, the absolute value.[9] In the Fermi gas model with equidistant spacing g^{-1}, the partial state density is given by[2]

$$\omega_n(E^*,\mathrm{p},\mathrm{h})=g\frac{(gE^*)^{n-1}}{\mathrm{p!h!}(n-1)!} \tag{3}$$

with a pairing correction to E^* for odd-even residual nuclei like ^{207}Bi. In view of the complete configuration mixing in the exciton model,[1] different values g for composite and residual nucleus may be justified and have been applied;[9,10] a consistent treatment of the hybrid model, however, requires one g value only.

For numerical calculations we have used the code ALICE/LIVERMORE 82 (Ref. 3) that includes a treatment of the equilibrated system according to Ewing and Weisskopf. For the parameters entering we have mostly used the optional[3] standard values; in particular, g has been given a value corresponding to a level density parameter $a=A/8.5$ MeV^{-1} (i.e., $a=24.5$ MeV^{-1} for $A=208$). For the precompound mode the geometry dependent version (GDH) that evaluates Eq. (1) for each partial wave separately has been applied.

The resulting spectra are compared in Fig. 2 with the experimental data. Agreement is only obtained in the evaporation region; the calculated PE continuum systematically underestimates the experimental result. The discrepancy increases from ^{204}Pb to ^{208}Pb and is of twofold character; it concerns firstly the magnitude and general shape—the experimental spectra are harder and the yield increases significantly with neutron excess—and secondly the lack of any structure for residual excitations $U<5$ MeV.

If this were an effect of the shell closure it should be taken care of in the hybrid model by using more realistic values for g. It is known from neutron resonance data[11] and from (n,n′) and (n,2n) reactions[12,13] with 14 MeV projectiles that the level density parameters a show a pro-

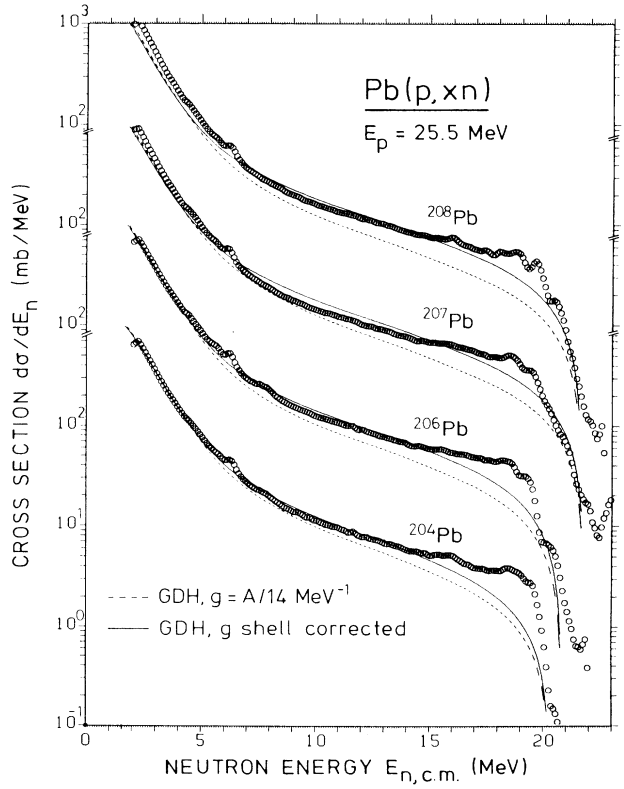

FIG. 2. Experimental (open circles) angle integrated neutron energy spectra compared to GDH model calculations with standard ($g=A/14$ MeV^{-1}, dashed line) and shell corrected (solid line) single particle level density.

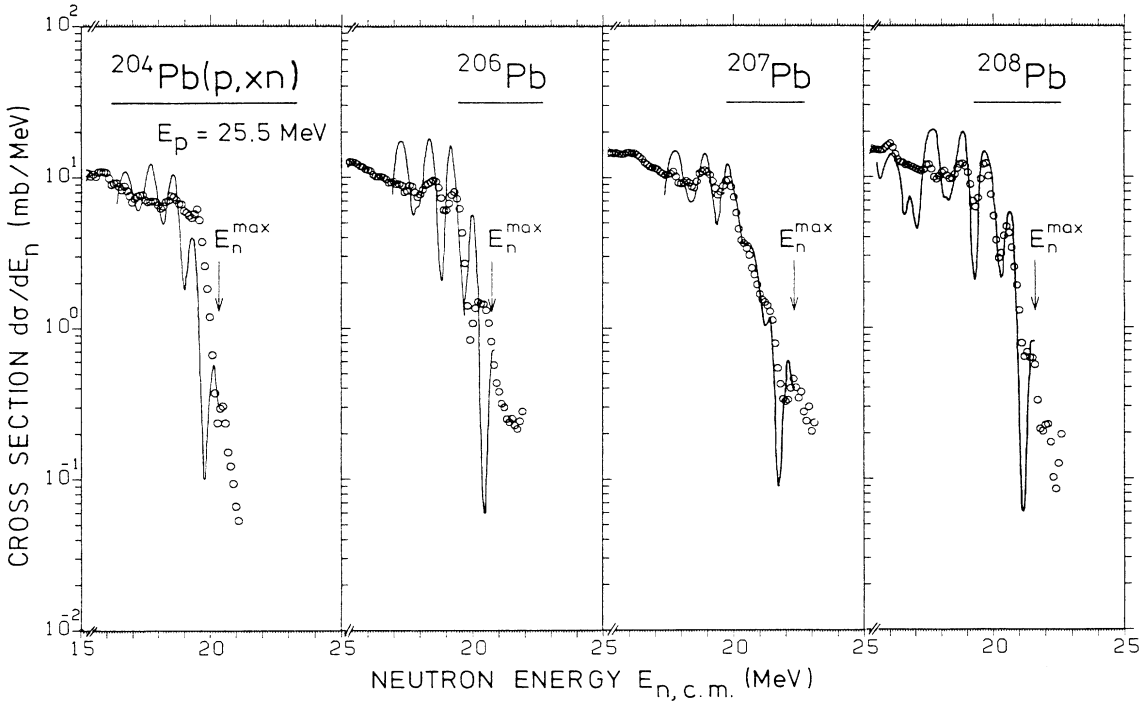

FIG. 3. High energy part of the Pb(p,n) spectra in the forward cone $\Theta_{lab} \leq 60°$. The solid line is the microscopically calculated $1p1n^{-1}$ state density. E_n^{max} denotes the kinematical limit.

nounced minimum near $A \approx 208$, in particular for the Pb and Bi isotopes and so will g. By adopting $a = 13$ MeV^{-1} for ^{208,209}Bi from Ref. 13 and extrapolating $a = 14$ (15;17) for ^{207}Bi (^{206}Bi;^{204}Bi) from Ref. 11 for determination of $g = 6a/\pi^2$ for the PE contribution, the calculations do indeed approach the experimental data in the PE region much better (Fig. 2) because $\lambda_c \propto g^{-1}$.

Of course, the spectral structure in the region $U \leq 5$ MeV cannot be accounted for with the smooth partial state densities of Eq. (3) that generates smooth spectra. Instead one can apply a microscopic approach[14] that starts from a set of single particle (s.p.) energies and generates the partial state densities for n excitons by means of a recursion relation.[4,5] For the projectile energy under discussion, the first term in Eq. (1) is by far dominant and contributes more than 90% of the yield for $E_n > 10$ MeV such that the spectral shape is entirely determined by the partial density $\omega_{n_0-1}(E^* - \epsilon_{s.p.}, 1, 1)$:

$$\frac{d\sigma(\epsilon_\nu)}{d\epsilon_\nu} \sim \omega_2(E^* - \epsilon_{s.p.}, 1, 1) \ . \tag{4}$$

We have performed the calculation of the one proton-particle one neutron-hole state density in the residual nuclei ^{204,206,207,208}Bi with the formalism described in Ref. 4, based on the realistic s.p. levels of the Nilsson model with the parameters of.[15] The nucleon pairing energies were those from,[16] the small ($\delta \leq 0.02$) deformation parameters from.[17] Finally, a slight energy smoothing was applied.

The results of this calculation are compared in Fig. 3 with those energy spectra obtained with high resolution in the forward cone $\Theta \leq 60°$, normalized to a solid angle 4π. The data show the structures much clearer than those of Fig. 2; the structure is most pronounced for ^{208}Bi, the nucleus with the $(1p)(1n)^{-1}$ deviation from closed shells. The calculations reproduce the general energy dependence as well as the structures in their positions reflecting the distribution of $(1p)(1n)^{-1}$ state strength (with a normalization in Eq. (4) of 1 mb/MeV $\hat{=}$ 45 states/MeV) very well up to 5 MeV of residual excitation U. It should be kept in mind that these structures appear in a region of high total level density that is, e.g., for ^{208}Bi and $U \approx 1.8$ MeV already on the order of 50 MeV^{-1}. Therefore Fig. 3 at the same time demonstrates the high selectivity of the PE mode in (p,n) reactions to $(1p)(1n)^{-1}$ states. The pairing gap for ^{207}Bi is reproduced, too. Obviously a stronger energy smoothing would also account for the experimental energy resolution and/or an increase of spreading width with increasing excitation or deformation.[4]

In summary, we have found evidence that strong deviations of single particle state densities from those of a Fermi gas influence the neutron PE emission in (p,n) reactions from nuclei as heavy as $^{204-208}_{83}$Bi. The general spectral shape of the PE continuum may be accounted for by lowering the s.p. level density g to values known from compound nucleus reactions at low excitation. The structures at the high energy end could be related to the nearby double shell closure; they correspond to the broader structures observed for sequences of nuclei crossing the $f_{7/2}$ or $g_{9/2}$ shell closure.[4,5] A more quantitative understanding will probably require the consideration of angular momentum coupling.

This work was funded by the German Federal Minister for Research and Technology (BMFT) under Contract 06 HH 175.

[1]J. Bisplinghoff, Phys. Rev. C **33**, 1569 (1986).
[2]F. C. Williams, Nucl. Phys. **A166**, 231 (1971).
[3]M. Blann and H. K. Vonach, Phys. Rev. C **28**, 1475 (1983).
[4]W. Scobel, M. Blann, T. T. Komoto, M. Trabandt, S. M. Grimes, L. F. Hansen, C. Wong, and B. A. Pohl, Phys. Rev. C **30**, 1480 (1984).
[5]M. Blann, S. M. Grimes, L. F. Hansen, T. T. Komoto, B. A. Pohl, W. Scobel, M. Trabandt, and C. Wong, Phys. Rev. C **32**, 411 (1985).
[6]Y. Holler, A. Kaminsky, B. Scharlemann, H. Krause, R. Langkau, W. Peters, G. Poppe, N. Schirm, W. Scobel, and R. Wien, Nucl. Instrum. Methods A **235**, 123 (1985).
[7]E. Mordhorst, M. Trabandt, A. Kaminsky, H. Krause, and W. Scobel, Phys. Rev. C **34**, 103 (1986).
[8]A. Kaminsky, Y. Holler, and W. Scobel, Nucl. Instrum. Methods A **244**, 443 (1986).
[9]J. M. Akkermans, H. Gruppelaar, and G. Reffo, Phys. Rev. C **22**, 73 (1980).
[10]H. Machner, G. Seniwongse, P. Jahn, M. Nolte, M. Rogge, and P. Turek, Phys. Rev. C **33**, 1931 (1986).
[11]W. Dilg, W. Schantl, H. K. Vonach, and M. Uhl, Nucl. Phys. **A217**, 269 (1973).
[12]L. F. Hansen, M. Blann, R. J. Howerton, T. T. Komoto, and B. A. Pohl, Nucl. Sci. Eng. **92**, 382 (1986).
[13]V. Schröder, W. Scobel, L. Wilde, and M. Bormann, Z. Phys. A **287**, 353 (1978).
[14]S. M. Grimes, *Proceedings of International Conference on Nuclear Data, Santa Fe, 1985,* edited by P. G. Young *et al.* (Gordon and Breach, New York, 1986), p. 995.
[15]P. A. Seeger and W. M. Howard, Nucl. Phys. **A238**, 491 (1975).
[16]A. Gilbert and A. G. W. Cameron, Can J. Phys. **43**, 1446 (1965).
[17]S. Åberg, Phys. Scr. **25**, 23 (1982).